salt of 5'-GMP. The data available for ordered association of the sodium salt of 5'-GMP most strongly support the octamer model, and this structure appears most consistent with the data for GDP and GTP. In particular, the existence of two equilibria for GDP and GTP is inconsistent with the helical association model, which would be envisioned as involving stepwise additions of nucleotide units held together by hydrogen bonding. The data indicating initial formation of stacked nucleotide dimers at low concentrations followed by a hydrogen-bonding association of dimers at concentrations greater than 190 mM are also consistent with the observation that highly ordered octameric units of GMP are not detected until nucleotide concentrations of 190 mM are reached[7] and, furthermore, explain the inability of others to observe tetrameric units.

In summary, base stacking of guanosine nucleotides is the primary self-associative process of low-concentration solutions (<100 mM) occurring at 25 °C. This association appears to be insensitive to the number of phosphate groups. A stacking pattern consistent with the data has the purine rings lying head to tail with the N-9 atoms on the same edge of the stack. The phosphate chain is the primary site of interaction of the guanosine nucleotides with manganous ion, and N-7 is the likely secondary site of association. At nucleotide concentrations greater than 190 mM we propose that stacked guanosine nucleotides associate by the formation of asymmetric hydrogen bonds to form octameric units.

Acknowledgment. We thank the National Institutes of Health (GM 25668-01) for support of this work and the Dreyfus Foundation for support of the purchase of the JEOL spectrometer used for many of the studies.

Registry No. GDP, 146-91-8; GTP, 86-01-1; manganous ion, 16397-91-4.

X-ray Structure Analyses and Vibrational Spectral Measurements of the Model Compounds of the Liquid-Crystalline Arylate Polymers. Finding Out the Raman Bands Characteristic of the Twisted Biphenyl Structure in Association with the Solid-to-Liquid Crystalline Phase Transition

Kohji Tashiro,*,† Jian-an Hou,† Masamichi Kobayashi,† and Toshihide Inoue‡

Contribution from the Department of Macromolecular Science, Faculty of Science, Osaka University, Toyonaka, Osaka 560, Japan, and The Research Association of Polymer Basic Technology, Toranomon, Kanda, Tokyo 101, Japan. *Received January 11, 1990*

Abstract: X-ray structural analyses and Raman spectral measurements have been made for two crystal modifications of the model compound of the liquid-crystalline arylate polymers: $EtOCOPhOCO(Ph)_2COOPhCOOEt$. The crystal data determined at room temperature for the α and β forms are as follows: α, monoclinic, $Pn\text{-}C^2_s$, a = 32.620 (5) Å, b = 5.847 (1) Å, c = 14.115 (2) Å, β = 98.19 (1)°, Z = 4, R = 0.057; β, monoclinic, $P2_1/c\text{-}C^5_{2h}$, a = 29.491 (4) Å, b = 5.4405 (3) Å, c = 8.3375 (8) Å, β = 94.890 (8)°, Z = 2, R = 0.072. The main difference in the molecular conformation between these two crystalline forms is a torsional angle between the two benzene rings of the biphenyl group: 48° for the α form and 0° for the β form. This conformational difference correlates to the difference in the characteristic Raman spectral pattern. For example, the 420- and 320-cm^{-1} Raman bands are observed only for the α form and can be utilized as a useful index for the twisted structure of the biphenyl group. The α form was found to transform into the β form at ca. 110 °C and then into the liquid-crystalline state (LC) at ca. 185 °C. The 420- and 320-cm^{-1} Raman bands disappeared in the α-to-β transition and reappeared in the β-to-LC transition, suggesting that the biphenyl group takes a twisted structure in the liquid-crystalline state as well as in the α crystal.

Recently a large amount of attention has been paid to the liquid-crystalline arylate polymers such as poly-*p*-oxybenzoyl, its copolymers with polyethylene terephthalate, etc., because of their excellent mechanical properties of high Young's modulus, high strength, and good processability.[1] These polymers experience a crystal-to-liquid crystal-phase transition at high temperature.[2] Spinning from the liquid-crystalline phase is one of the important processes to produce the mechanically strong fiber. Then it is required to clarify what type of structural change may occur during this phase transition. In general, however, the liquid-crystalline polymers show the very poor X-ray fiber patterns with quite a small number of broad reflections, making it practically impossible to perform the detailed structural analyses. In such a situation, a utilization of the model compounds may provide us with a chance to obtain a variety of useful information concerning the structural changes occurring in the phase transition of the liquid-crystalline polymers.

We have been studying a relationship between the crystal structure and the vibrational spectra of the following series of the model compounds so as to find out some important and useful indices necessary for clarifying the structure of the liquid-crystalline state. In the present study, the compound with n = 2 has

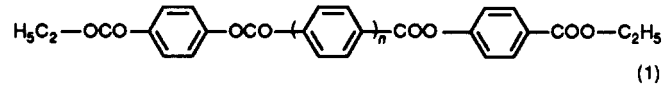

(1)

been selected which serves as a model for the liquid-crystalline

† Osaka University.
‡ The Research Association of Polymer Basic Technology.

(1) Chung, T. *Polym. Eng. Sci.* **1986**, *26*, 901.
(2) Varshney, S. K. *J. Macromol. Sci.—Rev. Macromol. Chem. Phys.* **1986**, *C26*, 551.

0002-7863/90/1512-8273$02.50/0

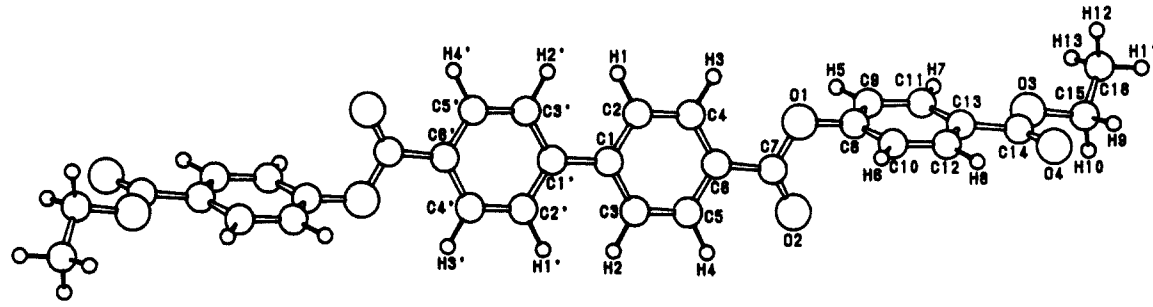

Figure 1. Molecular structure of the crystal form β.

arylate polymers containing the biphenyl group within the skeletal chains. This compound has been found to crystallize into two types of crystal modification, i.e., the α and β forms. The X-ray structure analysis has revealed a large difference in the molecular conformation, especially in the torsional angle of the biphenyl group, between these two modifications. The α form experiences a thermally induced phase transition to the β form at ca. 110 °C. Corresponding to the large structural change occurring in this transition, a remarkable change has been observed in the infrared and Raman vibrational spectral patterns. The thus observed explicit relationship between the molecular conformation and the spectral feature is considered useful as an important guide for understanding the structural feature of the liquid-crystalline state.

Experimental Section

X-ray Structural Determination. Single crystals of the modifications α and β were obtained from a slow evaporation of toluene solution at room temperature. The shape of the α crystal is pseudorectangular with the dimensions of 0.5 × 0.3 × 0.1 mm^3. The β crystal is the lozenge-type platelet with the dimensions of 0.2 × 0.2 (edges) × 0.1 (thickness) mm^3. The X-ray diffraction data were collected at room temperature by a Rigaku AFC-5 four-circle diffractometer installed at the Laboratory of X-ray Analysis in the Research Center for Protein Engineering, Osaka University, Japan. A graphite-monochromatized Cu K_α radiation (λ = 1.54178 Å) was used as an incident X-ray source (40 kV, 200 mA). The unit cell dimensions were determined by a least-squares fitting method for the 20 reflections within 36° < 2θ < 45° (α form) and the 19 reflections within 35° < 2θ < 41° (β form). Intensity data were collected by 2θ-ω scan mode with maximal 2θ of 120° for the α form and 125° for the β form. Scan width was $\Delta\omega = (1.0 + 0.15\tan\theta)°$. Backgrounds were counted for 4 s before and after each scan. Three standard reflections were recorded after every 100 scans, and no significant intensity variation was observed. For the α crystal, a total of 4628 independent reflections were collected in the region of h = −37 to 37, k = 0 to 6, and l = 0 to 16 at a rate of 4°(2θ) min^{-1}. For the β crystal, 2574 reflections were recorded for h = −33 to 33, k = 0 to 6, and l = 0 to 9 with a scan rate of 3°(2θ) min^{-1}. Of the total reflections, 2877 and 1492 significant reflections with $|F_o| \geq 3\sigma(|F_o|)$ were used, respectively, in the calculations of the structure factors.

The initial structures were searched by a program MULTAN-78[3] and refined by a program HBLS-V.[4] The quantity minimized by the HBLS-V was $\Sigma w(|F_o| - |F_c|)^2$, where $|F_o|$ and $|F_c|$ are the amplitudes of the observed and calculated structure factors, respectively, and $w = (\sigma(F_o)^2 + a|F_o| + b|F_o|^2)^{-1}$. After the R-factor was reduced to some extent by the thermally isotropic refinement, all the non-hydrogen atoms were then refined with anisotropic temperature factors. In the process of the least-squares refinement, the internal parameters of the molecules such as the bond length, bond angle, etc. were controlled so as to reserve the molecular geometry as reasonably as possible by referring to the standard values. As for the hydrogen atoms, the isotropic temperature factors were refined. Final reliability factors were R = 0.057 and R_w = 0.073 for the α form and R = 0.072 and R_w = 0.140 for the β form. The coefficients a and b in the above-defined weight w were 0.02096 and 0.00133 for the α form and 0.0 and 0.02540 for the β form, respectively. Atomic scattering factors were taken from the *International Tables for X-ray Crystallography*.[5]

(3) Main, P.; Hull, S. E.; Lessinger, L.; Germain, G.; Declercq, J. P.; Woolfson, M. M. MULTAN 78. A System of Computer Programs for the Automatic Solution of X-ray Diffraction Data. Universities of York, England and Louvain, Belgium, **1978**.

(4) Ashida, T. The Universal Crystallographic Computing System—Osaka, p 53. The Computation Center, Osaka University, Japan, **1973**.

(a)

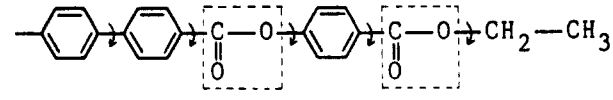

		τ_1	τ_2	τ_3	τ_4	τ_5
α Form						
Molecule	A	48	11	62	7	−174
			5	56	5	178
	B	47	11	59	8	−173
			3	55	6	−177
β Form		0	8	75	2	138

(b)

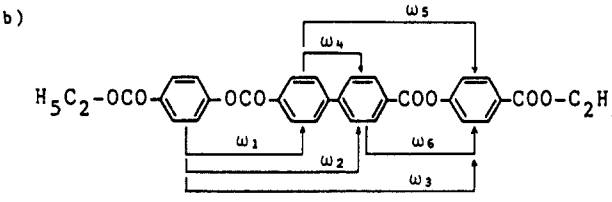

		ω_1	ω_2	ω_3	ω_4	ω_5	ω_6
α Form							
Molecule	A	49	4	51	48	4	50
	B	48	3	51	47	5	51
β Form		67	67	0	0	67	67

Figure 2. (a) Dihedral angles (deg) about the ring-ester and ring-ring linkages for the crystal forms α and β. In the α molecules, the corresponding dihedral angles in the right and left half parts of the chains are listed in the same columns. (b) Dihedral angles (deg) for the pairs of the benzene planes separated in space.

Raman Spectroscopic Measurements. Raman spectra were measured at the various temperatures by using a Japan Spectroscopic Company R-500 Raman spectrophotometer. The 514.5-nm line from an Ar^+ gas laser was used as an excitation light source. Both the single crystals and the powder samples were employed in the measurements. The powder samples were obtained by grinding a piece of single crystals with a definitely identified crystal form.

Results and Discussion

Molecular and Crystal Structures of the β Form. Crystal data of the β form were determined as follows: monoclinic, space group $P2_1/c$-C^5_{2h}, a = 29.491 (4) Å, b = 5.4405 (3) Å, c = 8.3375 (8) Å, β = 94.890 (8)°, V = 1332.9 (2) Å^3, Z = 2, d_x = 1.341 g/cm^3, F(000) = 564. In Figure 1 is shown the molecular structure of the β form. The fractional coordinates, the anisotropic temperature factors B_{ij} and the equivalent isotropic temperature factors (B_{eq}) of the atoms are available as supplementary material. The bond lengths and bond angles are given in Table I. Some of the torsional angles about the ring-ring and ring-ester linkages are shown in Figure 2. The benzene rings of the biphenyl group are coplanar with the torsional angle of about 0°. The ethyl ester group at the end of the chain has a gauche-type conformation with the dihedral angle (C–O–CH_2–CH_3) of ca. 137°. The crystal

(5) *International Tables for X-ray Crystallography*; Kynoch Press: Birmingham, England, **1974**; *Vol. IV*.

Table I. Bond Lengths and Bond Angles with Their Estimated Standard Deviations for the Crystal Form β

bond[a]	length, Å	bond	length, Å
C(1)–C(1′)	1.489 (7)	C(8)–C(9)	1.384 (6)
C(1)–C(2)	1.398 (6)	C(8)–C(10)	1.375 (6)
C(1)–C(3)	1.386 (6)	C(9)–C(11)	1.382 (6)
C(2)–C(4)	1.393 (6)	C(10)–C(12)	1.376 (6)
C(3)–C(5)	1.378 (6)	C(11)–C(13)	1.383 (6)
C(4)–C(6)	1.377 (6)	C(12)–C(13)	1.404 (6)
C(5)–C(6)	1.377 (6)	C(13)–C(14)	1.489 (6)
C(6)–C(7)	1.480 (6)	O(3)–C(14)	1.305 (6)
O(1)–C(7)	1.340 (5)	O(4)–C(14)	1.205 (6)
O(2)–C(7)	1.195 (7)	O(3)–C(15)	1.490 (9)
O(1)–C(8)	1.403 (5)	C(15)–C(16)	1.419 (10)
bond	**angle (deg)**	**bond**	**angle (deg)**
C(1′)–C(1)–C(2)	121.1 (4)	O(1)–C(8)–C(10)	119.7 (4)
C(1′)–C(1)–C(3)	121.7 (4)	C(9)–C(8)–C(10)	122.5 (4)
C(2)–C(1)–C(3)	117.2 (4)	C(8)–C(9)–C(11)	118.9 (4)
C(1)–C(2)–C(4)	121.4 (4)	C(8)–C(10)–C(12)	118.5 (4)
C(1)–C(3)–C(5)	121.2 (4)	C(9)–C(11)–C(13)	119.6 (4)
C(2)–C(4)–C(6)	119.8 (4)	C(10)–C(12)–C(13)	120.0 (4)
C(3)–C(5)–C(6)	121.1 (4)	C(11)–C(13)–C(12)	120.4 (4)
C(4)–C(6)–C(5)	119.1 (4)	C(11)–C(13)–C(14)	122.5 (4)
C(4)–C(6)–C(7)	123.4 (4)	C(12)–C(13)–C(14)	117.1 (4)
C(5)–C(6)–C(7)	117.5 (4)	C(13)–C(14)–O(3)	112.4 (4)
C(6)–C(7)–O(1)	113.2 (4)	C(13)–C(14)–O(4)	124.3 (4)
C(6)–C(7)–O(2)	124.7 (4)	O(3)–C(14)–O(4)	123.2 (5)
O(1)–C(7)–O(2)	122.1 (4)	C(14)–O(3)–C(15)	117.1 (4)
C(7)–O(1)–C(8)	116.9 (3)	O(3)–C(15)–C(16)	109.0 (6)
O(1)–C(8)–C(9)	117.8 (3)		

[a] Numbering of the atoms is referred to in Figure 1.

structure of the β form is shown in Figure 3. The molecules are packed in a two-dimensional layer structure, and the layers are stacked together along the a axis. The molecular axes are tilted by about 13° from the normal to the plane within the plane of (010). The chains are packed side by side in such a way that the benzene or ester groups are arranged in the same height but with an opposite sense.

Molecular and Crystal Structures of the α Form. The crystal data of the α crystal form is listed below: monoclinic, space group Pn-C^2_s, a = 32.620 (5) Å, b = 5.847 (1) Å, c = 14.115 (2) Å, β = 98.19 (1)°, V = 2664.9 (7) Å^3, Z = 4, d_x = 1.342 g/cm^3, $F(000)$ = 1128. The finally obtained fractional coordinates and the anisotropic and equivalent isotropic temperature factors of the atoms are available as supplementary material. One crystallographically asymmetric unit consists of two independent molecules A and B, the molecular conformations of which are shown in Figure 4. The bond lengths and bond angles are listed in Tables II and III, respectively. As seen in Figure 4 and Tables II and III, the molecular conformations of the A and B chains

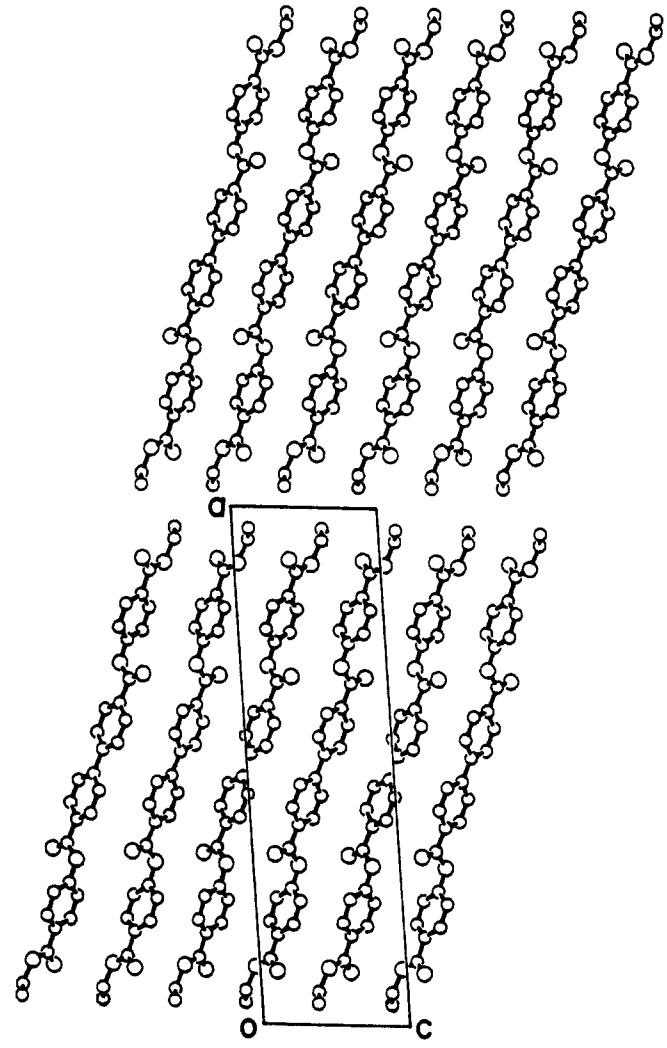

Figure 3. Crystal structure projected along the b axis of the crystal form β.

Table II. Bond Lengths and Their Estimated Standard Deviations for the Crystal Form α

	length (Å)			length (Å)	
bond[a]	molecule A	molecule B	bond[a]	molecule A	molecule B
C(1)–C(2)	1.554 (13)	1.470 (16)	C(17)–C(18)	1.394 (10)	1.377 (11)
C(2)–O(1)	1.475 (12)	1.421 (13)	C(17)–C(19)	1.386 (10)	1.425 (12)
O(1)–C(3)	1.391 (9)	1.315 (10)	C(18)–C(20)	1.403 (10)	1.435 (11)
C(3)–O(2)	1.186 (9)	1.221 (10)	C(19)–C(21)	1.392 (10)	1.385 (11)
C(3)–C(4)	1.508 (10)	1.495 (11)	C(20)–C(22)	1.429 (10)	1.394 (10)
C(4)–C(5)	1.352 (9)	1.429 (11)	C(21)–C(22)	1.430 (11)	1.406 (9)
C(4)–C(6)	1.393 (10)	1.407 (11)	C(22)–C(23)	1.458 (10)	1.503 (9)
C(5)–C(7)	1.392 (9)	1.388 (11)	C(23)–O(5)	1.340 (8)	1.377 (8)
C(6)–C(8)	1.399 (10)	1.370 (10)	C(23)–O(6)	1.185 (9)	1.167 (8)
C(7)–C(9)	1.362 (10)	1.417 (10)	O(5)–C(24)	1.437 (9)	1.391 (8)
C(8)–C(9)	1.370 (10)	1.392 (9)	C(24)–C(25)	1.380 (12)	1.402 (11)
C(9)–O(3)	1.395 (8)	1.386 (8)	C(24)–C(26)	1.399 (11)	1.394 (11)
O(3)–C(10)	1.358 (10)	1.346 (9)	C(25)–C(27)	1.386 (11)	1.419 (11)
C(10)–O(4)	1.217 (11)	1.205 (10)	C(26)–C(28)	1.363 (11)	1.399 (11)
C(10)–C(11)	1.455 (12)	1.482 (10)	C(27)–C(29)	1.392 (11)	1.398 (11)
C(11)–C(12)	1.361 (11)	1.369 (9)	C(28)–C(29)	1.382 (11)	1.436 (11)
C(11)–C(13)	1.413 (11)	1.384 (9)	C(29)–C(30)	1.484 (14)	1.466 (11)
C(12)–C(14)	1.412 (10)	1.382 (10)	C(30)–O(7)	1.339 (13)	1.313 (9)
C(13)–C(15)	1.356 (10)	1.381 (9)	C(30)–O(8)	1.226 (14)	1.220 (10)
C(14)–C(16)	1.369 (9)	1.395 (10)	O(7)–C(31)	1.458 (16)	1.442 (9)
C(15)–C(16)	1.412 (10)	1.372 (9)	C(31)–C(32)	1.591 (26)	1.560 (13)
C(16)–C(17)	1.475 (10)	1.535 (10)			

[a] Numbering of the atoms is referred to in Figure 4.

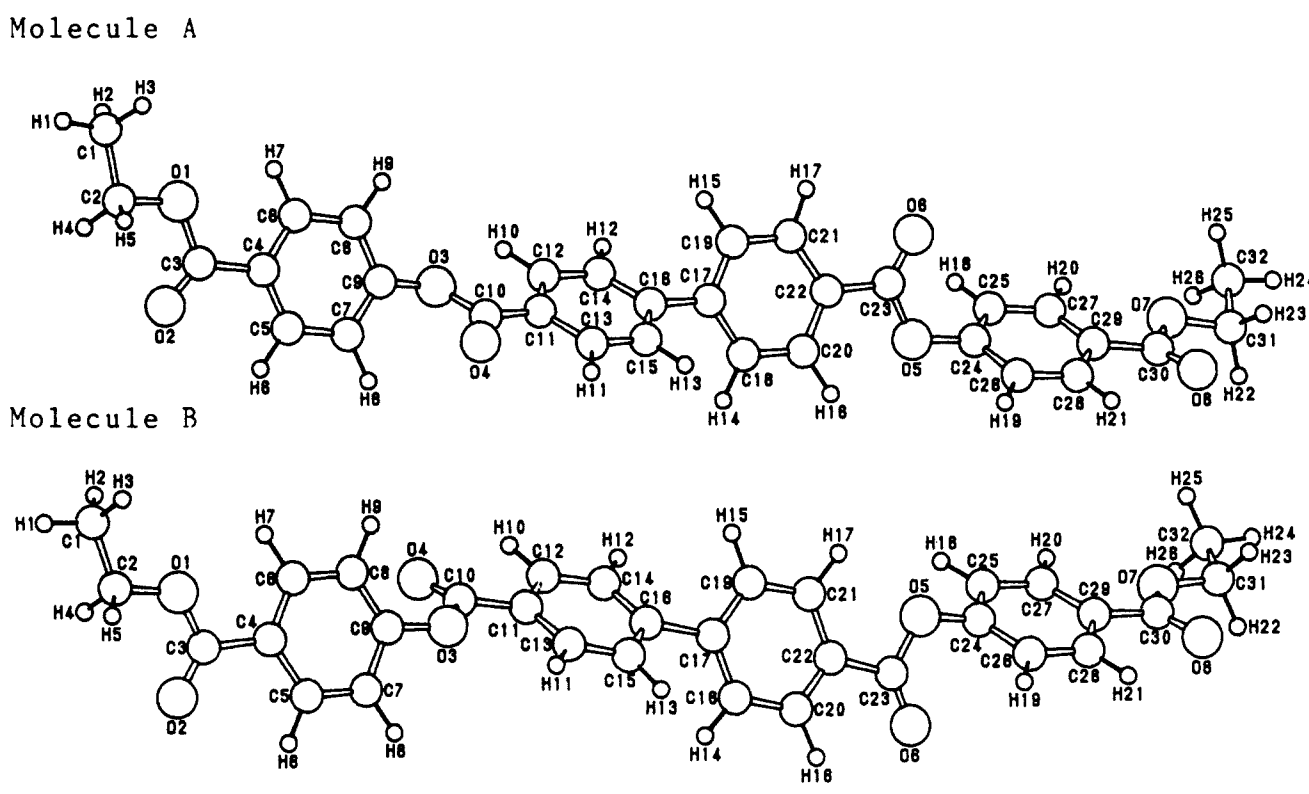

Figure 4. Structure of the A and B molecules of the crystal form α.

Table III. Bond Angles and Their Estimated Standard Deviations for the Crystal Form α

bond[a]	angle (deg) molecule A	angle (deg) molecule B	bond[a]	angle (deg) molecule A	angle (deg) molecule B
C(1)-C(2)-O(1)	100.8 (7)	113.8 (9)	C(16)-C(17)-C(18)	121.1 (6)	119.1 (7)
C(2)-O(1)-C(3)	109.0 (6)	122.2 (7)	C(16)-C(17)-C(19)	119.8 (6)	119.7 (7)
O(1)-C(3)-C(4)	114.2 (6)	112.9 (7)	C(18)-C(17)-C(19)	119.1 (7)	121.2 (7)
O(1)-C(3)-O(2)	120.5 (7)	120.2 (8)	C(17)-C(18)-C(20)	121.7 (7)	119.1 (7)
O(2)-C(3)-C(4)	124.5 (7)	125.9 (7)	C(17)-C(19)-C(21)	121.5 (7)	119.3 (8)
C(3)-C(4)-C(5)	118.5 (6)	118.9 (7)	C(18)-C(20)-C(22)	118.9 (6)	119.3 (7)
C(3)-C(4)-C(6)	119.1 (6)	120.3 (7)	C(19)-C(21)-C(22)	120.0 (7)	120.0 (7)
C(5)-C(4)-C(6)	122.3 (6)	120.6 (7)	C(20)-C(22)-C(21)	118.5 (7)	120.6 (6)
C(4)-C(5)-C(7)	119.0 (6)	120.2 (7)	C(20)-C(22)-C(23)	122.4 (7)	117.0 (6)
C(4)-C(6)-C(8)	118.3 (7)	119.2 (7)	C(21)-C(22)-C(23)	118.9 (7)	122.4 (6)
C(5)-C(7)-C(9)	119.3 (6)	117.3 (7)	C(22)-C(23)-O(5)	110.3 (6)	107.9 (5)
C(6)-C(8)-C(9)	118.6 (7)	120.1 (7)	C(22)-C(23)-O(6)	125.0 (7)	123.5 (6)
C(7)-C(9)-C(8)	122.4 (7)	122.5 (6)	O(5)-C(23)-O(6)	124.7 (6)	128.5 (6)
C(7)-C(9)-O(3)	120.9 (6)	114.1 (6)	C(23)-O(5)-C(24)	117.2 (6)	117.0 (5)
C(8)-C(9)-O(3)	115.5 (6)	123.4 (6)	O(5)-C(24)-C(25)	119.6 (7)	113.9 (6)
C(9)-O(3)-C(10)	122.6 (6)	120.5 (6)	O(5)-C(24)-C(26)	118.7 (7)	123.2 (6)
O(3)-C(10)-C(11)	113.7 (7)	114.1 (6)	C(25)-C(24)-C(26)	121.7 (7)	122.9 (7)
O(3)-C(10)-O(4)	118.1 (8)	120.4 (7)	C(24)-C(25)-C(27)	118.3 (8)	118.6 (7)
O(4)-C(10)-C(11)	128.2 (8)	125.2 (7)	C(24)-C(26)-C(28)	119.4 (7)	118.3 (7)
C(10)-C(11)-C(12)	124.4 (8)	117.1 (6)	C(25)-C(27)-C(29)	119.9 (7)	119.9 (7)
C(10)-C(11)-C(13)	116.2 (7)	122.7 (6)	C(26)-C(28)-C(29)	119.6 (8)	120.4 (7)
C(12)-C(11)-C(13)	119.4 (7)	120.2 (6)	C(27)-C(29)-C(28)	121.0 (7)	119.8 (7)
C(11)-C(12)-C(14)	119.3 (7)	119.9 (6)	C(27)-C(29)-C(30)	120.8 (8)	123.4 (7)
C(11)-C(13)-C(15)	120.6 (7)	120.5 (6)	C(28)-C(29)-C(30)	118.1 (8)	116.8 (7)
C(12)-C(14)-C(16)	122.0 (6)	119.4 (6)	C(29)-C(30)-O(7)	112.5 (9)	113.5 (6)
C(13)-C(15)-C(16)	121.2 (6)	118.9 (6)	C(29)-C(30)-O(8)	120.3 (10)	122.0 (7)
C(14)-C(16)-C(15)	117.5 (6)	120.8 (6)	O(7)-C(30)-O(8)	126.0 (10)	124.3 (7)
C(14)-C(16)-C(17)	121.8 (6)	120.7 (6)	C(30)-O(7)-C(31)	110.5 (9)	117.7 (6)
C(15)-C(16)-C(17)	120.8 (6)	118.4 (6)	O(7)-C(31)-C(32)	98.0 (12)	108.2 (6)

[a] Numbering of the atoms is referred to in Figure 4.

are very similar to each other. The torsional angle of the benzene–benzene linkage in the biphenyl group is 48.4° for the A molecule and 47.1° for the B molecule. The torsional angles about the benzene–ester linkages are listed in Figure 2. The ethyl ester groups at the ends of the chain have the trans conformation (173 and 178°) both for the A and B molecules. The detailed comparison in the molecular structure between the α and β forms will be made in the next section. As shown in Figure 5, the molecules form a stacked layer structure, and the layers are packed together in parallel to the (200) planes. The molecular chains are arranged in a layer with their long axes tilted by ca. 59° from the normal to the layer surface and by ca. 4° from the (010) plane.

A Difference in Molecular Conformation between the α and β Forms. In Figure 2 are compared the internal rotational angles around the skeletal bonds between the crystal forms α and β. As stated already, the molecules A and B of the α form exhibit a very similar set of the internal rotational angles with each other. Except for the biphenyl group (τ_1) and the end ethyl ester group (τ_5),

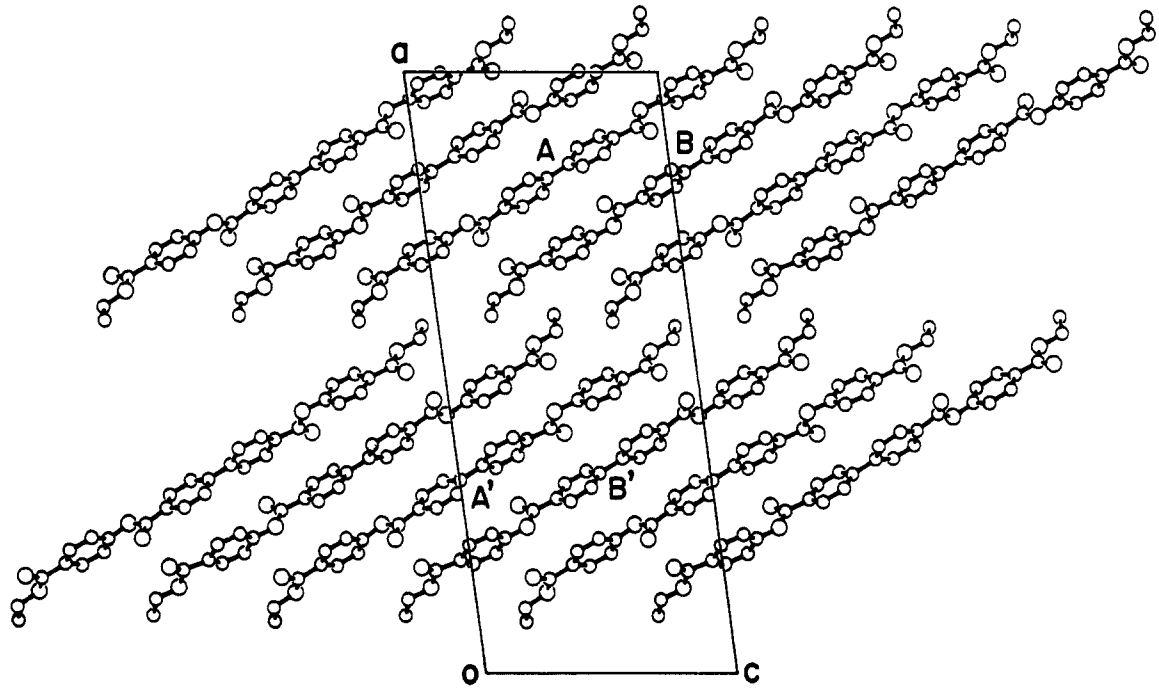

Figure 5. Crystal structure projected along the *b* axis of the crystal form α.

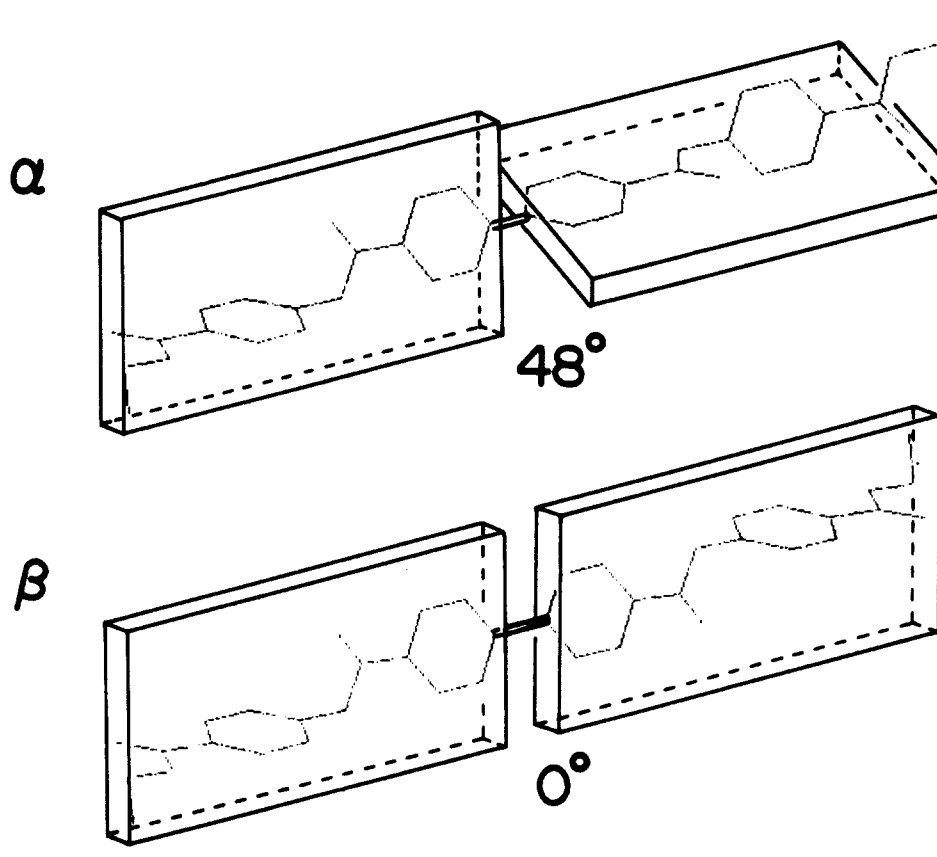

Figure 6. A schematic illustration of the essences of the conformational difference between the α and β forms, where the boards represent the parts of PhCOOPhCOOEt.

the molecular conformations of the α and β forms are also not very different from each other. That is to say, the molecular chains may be assumed as a linear connection of the two sheets of the board with a specific conformation common to the α and β forms (see Figure 6). These two sheets of the board make the dihedral angle of 0°(β) or 48°(α). As seen in the reported X-ray structure data[6-12] and in the present results, the biphenyl group takes the various values of the internal rotation angle depending on the variation in the environmental conditions or the intermolecular interactions. In other words, the biphenyl ring has a comparatively low-energy barrier in the ring–ring internal rotation potential as

(6) Trotter, J. *Acta Crystallogr.* **1961**, *14*, 1135.
(7) Hargreaves, A.; Rizvi, S. H. *Acta Crystallogr.* **1962**, *15*, 365.
(8) Boonstra, E. G. *Acta Crystallogr.* **1963**, *16*, 816.
(9) Charbonneau, G.-P.; Delugeard, Y. *Acta Crystallogr.* **1977**, *B33*, 1586.
(10) Kronebusch, P.; Gleason, W. B.; Britton, D. *Cryst. Struct. Commun.* **1976**, *5*, 839.
(11) Brock, C. P.; Kuo, M.-S. *Acta Crystallogr.* **1978**, *B34*, 981.
(12) Brock, C. P. *Acta Crystallogr.* **1980**, *B36*, 968.

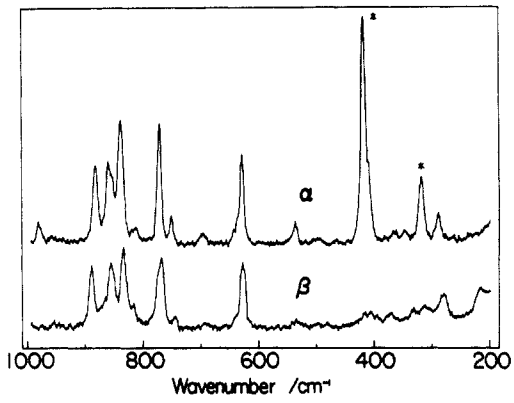

Figure 7. Raman spectra of the crystal forms α and β measured at room temperature.

pointed out in many papers.[13-18] The same situation can be seen also in the present case: the molecular packing of the α and β forms is different from each other (compare Figures 3 and 5), reflecting on the difference in the torsional angle of the biphenyl structure (Figure 2). The energy calculation is now being carried out so as to clarify to what extent the intramolecular and intermolecular interactions affect the twisted structure of the biphenyl parts in the α and β forms.

A Close Relationship between the Molecular Structure and the Vibrational Spectra. As stated above, the α and β forms are different in the internal rotational angle of the biphenyl group (Figure 6). Such a difference has been found to reflect directly on the infrared and Raman spectral patterns. For example, Figure 7 shows the Raman spectra of the powdered α and β crystal forms measured at room temperature in the frequency region of 200–1000 cm^{-1}. In the Raman spectrum of the α form, more numbers of the bands are observed than those for the β form in the frequency region of 200–4000 cm^{-1}, reflecting the lower symmetry of the α structure. Although many bands are observed almost in common to the α and β forms, some characteristic intense bands are detected uniquely in the spectra of the α form as indicated by asterisks. Especially, the bands at 420 and 320 cm^{-1} should be kept in mind. These bands are characteristic of the α form and may be assigned to the vibrational modes of the twisted biphenyl group. This assignment is based on the facts that (1) the essential difference in the molecular conformation between the α and β forms is the torsional angle of the biphenyl group (refer to Figure 6) and (2) these bands are unique for the biphenyl compounds and not observed for the arylate compounds containing only the isolated phenylene rings ($n = 1$ in the formula 1, for example[19]). In this way the close relation between the biphenyl conformation and the vibrational spectral pattern has been definitely proved here through the organized combination of the X-ray structural analysis and the spectroscopic measurements, being the first case in the structural studies of the biphenyl compounds as long as the authors have known. In order to confirm a universality of this relation, we measured the Raman spectra for the various biphenyl compounds with the twisted structures. In Figure 8 are reproduced the Raman spectra measured for *p*-dinitrobiphenyl (34° twisted[8]), *p*-dibromobiphenyl (42° twisted[10]), and the biphenyl itself in the solid (0°)[6,7,9] and in the benzene solution (22°:[13] strictly speaking, this value was reported for the biphenyl–*n*-hexane solution system. But the Raman spectrum is essentially the same in the benzene and *n*-hexane solutions.). Except for the case of the planar biphenyl, the intense band is observed around 420 cm^{-1} for all the substances presented in

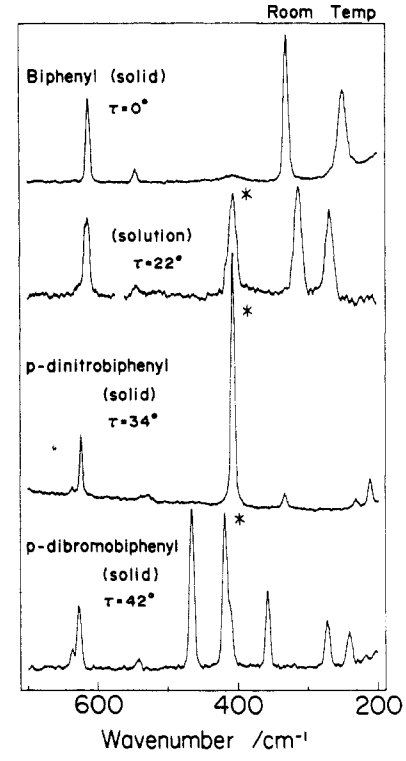

Figure 8. Raman spectra taken at room temperature for biphenyl (solid state and benzene solution), *p*-dinitrobiphenyl (solid state), and *p*-dibromobiphenyl (solid state) in the frequency region of 200–700 cm^{-1}.

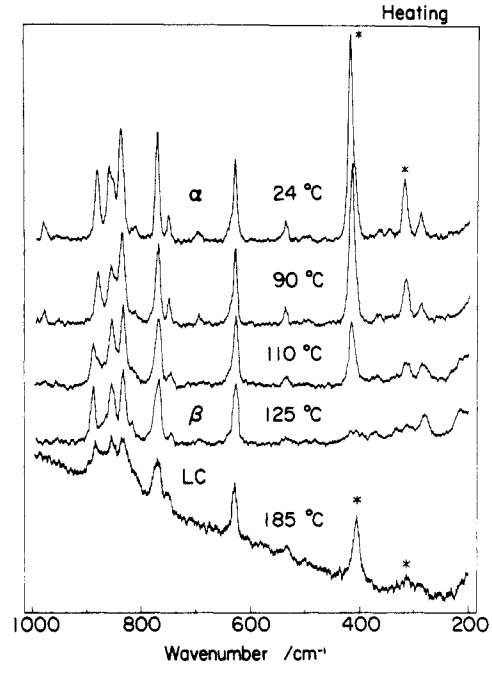

Figure 9. Temperature dependence of the Raman spectra measured for the crystal form α in the heating process.

Figure 8. In this way the characteristic bands in question may be generally said to be intrinsic of the twisted biphenyl structure and can be utilized as an important key for the detection of the twisted biphenyl structure in the various types of compounds.

In Figure 9 is shown the Raman spectral change measured in the transition process from the α form to the liquid-crystalline phase via the β form. The 420- and 320-cm^{-1} Raman bands change the intensity remarkably; the band intensity decreases down to zero in the α-to-β transition at about 110 °C and increases again in the transition from the β to the liquid-crystalline phase at about 185 °C. This indicates that the biphenyl group changes the conformation from the twisted form (α) to the planar form (β)

(13) Suzuki, H. *Bull. Chem. Soc. Jpn.* **1959**, *32*, 1340.
(14) Casalone, G.; Mariani, C.; Muguoli, A.; Simonetta, M. *Mol. Phys.* **1968**, *15*, 339.
(15) Huler, E.; Warshel, A. *Acta Crystallogr.* **1974**, *B30*, 1822.
(16) Carreira, L. A.; Towns, T. G. *J. Mol. Struct.* **1977**, *41*, 1.
(17) Akiyama, M.; Watanabe, T.; Kakihara, M. *J. Phys. Chem.* **1986**, *90*, 1752.
(18) Kirin, D. *J. Phys. Chem.* **1988**, *92*, 3691.
(19) Tashiro, K.; Hou, J.; Kobayashi, M. To be published.

and again to the twisted form in the liquid-crystalline state. By taking into account the low-energy barrier of the torsional potential, the biphenyl group is considered to experience a thermal motion, such as flip-flop motion of the benzene rings, in the high-temperature liquid-crystalline phase. The details of the molecular conformational change and the vibrational assignments will be reported in a separate paper.

Acknowledgment. The authors thank the Laboratory of X-ray Analysis in the Research Center for Protein Engineering, Osaka University, Japan for their kind permission to utilize the X-ray diffraction and structure analysis systems.

Supplementary Material Available: Tables of the fractional coordinates and temperature factors of the constituent atoms (4 pages); tables of the observed and calculated structure factors for the crystal forms α and β (17 pages). Ordering information is given on any current masthead page.

Detection of Alkyl, Alkoxyl, and Alkyperoxyl Radicals from the Thermolysis of Azobis(isobutyronitrile) by ESR/Spin Trapping. Evidence for Double Spin Adducts from Liquid-Phase Chromatography and Mass Spectroscopy

Edward G. Janzen,* Peter H. Krygsman, David A. Lindsay,† and D. Larry Haire

Contribution from the Department of Chemistry and Biochemistry, University of Guelph, Guelph, Ontario, N1G 2W1 Canada, and Division of Chemistry, National Research Council of Canada, 100 Sussex Drive, Ottawa, Ontario, K1A OR6 Canada. *Received February 15, 1990*

Abstract: The thermolysis of azobis(isobutyronitrile) (AIBN) in the presence of oxygen has been investigated by spin trapping by using α-phenyl *N-tert*-butyl nitrone (PBN) and 5,5-dimethylpyrroline *N*-oxide (DMPO). The aminoxyl products identified by ESR and mass spectroscopy (MS) are the result of trapping 2-cyano-2-propyl radicals (CP$^\bullet$) in the presence of oxygen. By low-temperature ESR the 2-cyano-2-propylperoxyl adduct of PBN-*nitronyl*-^{13}C is detectable in the presence of oxygen. The mass spectrum of the alkoxyl adduct is detectable only by the use of liquid chromatography/mass spectroscopy (LC/MS). The alkoxylamines, the *C*-(2-cyano-2-propyloxyl), *O*-(2-cyano-2-propyl) mixed double adducts of PBN (CPO-PBN-CP) and DMPO (CPO-DMPO-CP), have been observed for the first time. The normal double adducts, CP-PBN-CP or CP-DMPO-CP, are not detected.

Introduction

Some of the first nitrone spin trapping experiments published[1,2] involved the thermolysis of azobis(isobutyronitrile)[3] (AIBN), in the presence of α-phenyl *N-tert*-butyl nitrone (PBN) or 5,5-dimethylpyrroline *N*-oxide (DMPO). The ESR spectra obtained after thermolysis at 110 °C were consistent with the addition of the 2-cyano-2-propyl radical (CP$^\bullet$), to the nitrone to yield the corresponding aminoxyl spin adducts. Also reported[4,5] was the

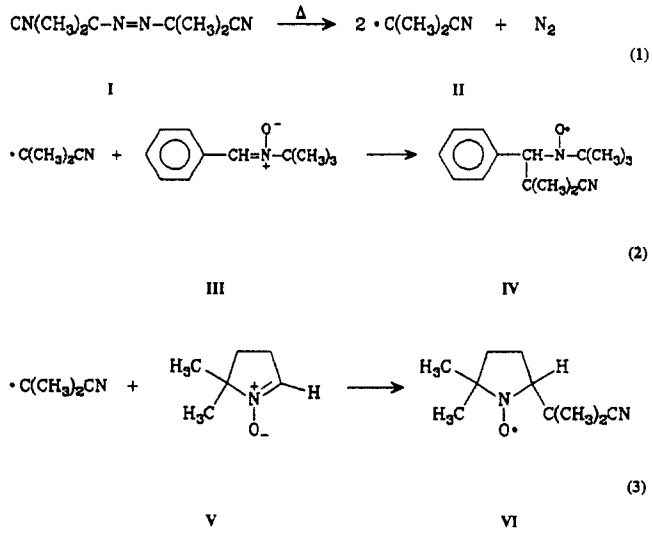

(1)

I II

(2)

III IV

(3)

V VI

* Author to whom correspondence should be addressed. New address: Departments of Clinical Studies and Biomedical Sciences, M.R.I. Facility, Ontario Veterinary College, University of Guelph, Guelph, Ontario, N1G 2W1 Canada.

† National Research Council of Canada.

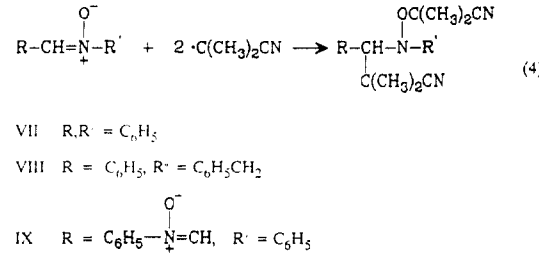

(4)

VII R,R$^\cdot$ = C_6H_5

VIII R = C_6H_5, R$^\cdot$ = $C_6H_5CH_2$

IX R = C_6H_5—N(O$^-$)=CH, R$^\cdot$ = C_6H_5

radical 1,3-addition to nitrones VII–IX, similar in structure to PBN, to produce the corresponding N,N,O-trisubstituted hydroxylamines (or alkoxylamines) when AIBN or other azo initiators were decomposed in xylene 90–110 °C. However no "double trapping" was reported for PBN or DMPO. It was therefore apparent that some nitrones react with certain radicals to give single adducts which are stable aminoxyls, while others give 1,3-addition products. CIDNP studies[6,7] of reacting systems later confirmed that 1,3-addition to the nitrone function proceeds with initial radical addition to the nitronyl carbon atom followed by a second radical–radical coupling at the oxygen atom of the aminoxyl intermediate.

Since the initial work by Iwamura and Inamoto,[1,2] spin trapping studies using PBN with AIBN as the radical source have subsequently described two different ESR spectra which have *both* been assigned to the 2-cyano-2-propyl radical adduct, (CP-PBN$^\bullet$)!

(1) Iwamura, M.; Inamoto, N. *Bull. Chem. Soc. Jpn.* **1967**, *40*, 703.
(2) Iwamura, M.; Inamoto, N. *Bull. Chem. Soc. Jpn.* **1970**, *43*, 860–863.
(3) Listed in *Chemical Abstracts* as propanenitrile; 2,2'-azobis[2-methyl].
(4) Iwamura, M.; Inamoto, N. *Bull. Chem. Soc. Jpn.* **1967**, *40*, 702.
(5) Iwamura, M.; Inamoto, N. *Bull. Chem. Soc. Jpn.* **1970**, *43*, 856–860.
(6) Iwamura, H.; Iwamura, M.; Tamura, M.; Shiomi, K. *Bull. Chem. Soc. Jpn.* **1970**, *43*, 3638.
(7) Iwamura, H.; Iwamura, M. *Tetrahedron Lett.* **1970**, *42*, 3723–3726.

0002-7863/90/1512-8279$02.50/0